IMAGE-BASED PASSENGER DETECTION AND LOCALIZATION INSIDE VEHICLES

Petko Faber
Institute of Photogrammetry, University of Bonn,
Nussallee 15, 53115 Bonn, Germany
npf@ipb.uni-bonn.de

Working Group V/III

KEY WORDS: intelligent airbag system, least squares method, ellipsoid.

ABSTRACT

In our paper we describe the ongoing research to develop an *intelligent airbag system*. Using image sequences acquired from a stereo camera, we detect the form and the position of the driver and passenger seat. And, if a seat is classified as occupied, we try to estimate the geometry and position of the human's head as the most distinguishing feature of the body, if it is possible.
The developed software system consists of five steps: the correction of distortions followed by an epipolar rectification of the stereo images, the feature extraction, the feature-based matching, the seat occupation detection and verification, and the approximation of the human's head. The emphasis in this paper is on the used model to approximate the human's head by an ellipsoid. The base of a subset of the estimated features as well as a certain assignment of the features to a human's head. The used model bases on the least square method with a condition, which supports the approximation of an ellipsoid. To determine, if an obtained approximation is valid the result is compared with the standard dimensions of a human's head. On tests on numerous image sequences recorded inside different vehicles the feasibility of the system is shown. The information about the seat occupation and the location of the detected passengers inside the vehicle can be used to control an intelligent airbag deployment.

Figure 1: Possible scenarios seen by a camera inside a vehicle, which are of special interest for an intelligent airbag deployment.

1 INTRODUCTION

Airbags can save or kill. Does your airbag know the difference? During the pre-crash braking, a passenger may be thrown against the dashboard area in immediate proximity to the airbag. On the other hand, an airbag inflates in less than 1/25th of a second. The energy required to inflate an airbag can seriously or even fatally insure driver and passenger who are too close to the airbag as they begin to inflate. It is important to understand that injuries occur because of passengers's positions when the airbag begins to deploy, not because of passengers's sizes or ages. Anyone on top of, or very close to, the airbag is at risk.

In (1) and (2) various aspects are reported about the effectiveness of occupant protection systems like safety belts and airbags and their use. The National Highway Traffic Safety Administration estimates that more than 4750 people are alive today because of their airbag. Driver deaths are being reduced by about 14 percent. But also 148 deaths are reported since 1990, caused by airbags which are deployed in low severity crashes. These deaths include 36 unbelted drivers, 4 unbelted

adult passengers, 68 children between the ages of 1 and 11, and 18 infants. Analyzing the causes of the reported deaths it can be deduced that the most adult victims are unbelted and the injured childs or infants are placed in the front seat of a vehicle with a passenger-side airbag. And so, three different scenarios can be defined, which are of a special interest for an intelligent airbag deployment:

1. the seat is occupied by a adult passenger, who is not belted (correctly) or not in a defined position on the seat,
2. the seat is occupied by a child or an infant (in a suitable child seat or rear-facing infant seat), or
3. the seat is empty or occupied by any other object e.g. a bag or a jacket.

In the last decade a lot of scientific groups focus their research to develop an *intelligent airbag system*. First solutions for passenger detection were already transferred into practice by different vehicle manufacturers. But, useful are systems which can *detect* and *localize* passengers inside a vehicle to protect the passengers.

The literature contains a lot of aproaches to detect humans in 2-D and 3-D (e. g. (Aggarwal and Cai, 1999, Gavrila, 1999, Krumm and Kirk, 1998)). However, often the approaches are model-driven, bases on colour informations (e. g. (Birchfeld, 1998, Fieguth and Terzopoulos, 1997, Sobottka and Pitas, 1996)) or the step of initialization works semi-automatically with restrictions on the persons position (e. g. (Schubert and Dickmanns, 1998, Yow and Cipolla, 1996)).

In this paper we describe the research effort to develop a system to detect and localize driver and passenger inside vehicles. Our system reliably classifies a seat as either empty or occupied. If a seat is occupied we try to detect and localize the passengers's head in 3-D. The main problem is, that we do not not know *whether* and *where* passengers are inside the vehicle. A sensor in the passenger seat which recognizes if the seat is occupied or not is not available. Furthermore the integration of a movement detection as additional feature is not possible, since a (significant) movement of a person cannot be assumed inevitably (e. g. sleeping passengers or children, which are limited in their freedom of movement by a child seat). We need to localize also such passengers. And last but not least, to make the system attractive for an integration in a vehicle, the costs are to be kept as low as possible, which affects also the used hardware components. Concretely, we can not use colour cameras.

In section 2 we describe the used experimental setup and the developed computational structure. The step of passenger detection and localization is described in detail in section 3. And finally, in section 4 the feasibility of the approach is shown.

2 STEREO CAMERA SYSTEM

2.1 Experimental setup

The used experimental setup (cf. fig. 2) consists of two b/w cameras with wide angle objectives. The sensor system is mounted at the windshield close to the driving mirror. Other positions to mount the sensor system inside the vehicle are possible, but are usually not accepted by the car designers.
To take the image sequences we use only the existing lighting. Other approaches, such as infrared, radar, and ultrasonic are hampered by severe problems, e.g. legality, accuracy, and electronic smog. Also no structuring lighting is used. The size of the stereo images we use at the moment is 360×288 [pels].

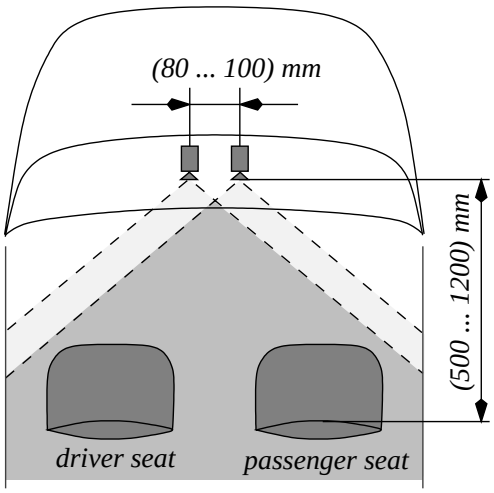

Figure 2: Used eperimental setup for binocular images of vehicles' interior

2.2 Computational structure

The developed computational structure consists of the following steps: 1) the correction of distortions followed by an epipolar rectification of a stereo image pair, 2) a feature extraction, 3) a feature-based matching, 4) the detection and verification of the seat occupation, and 5) finally the detection and localization of passengers.

The `input` of the developed software system are stereo image sequences and a set of calibration parameters. The `output` is defined by the information about the status of the seat occupation.

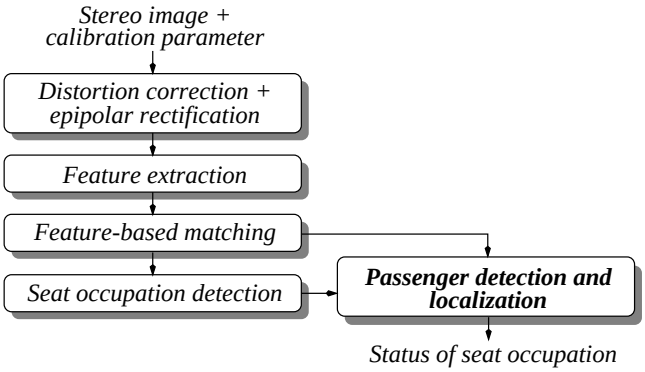

Figure 3: Computational structure.

Distortion correction and epipolar rectification: The `input` of this module is defined by stereo images and the calibration parameters. The calibration of the stereo system is a priori done by a test field based camera calibation performed off-line. The `output` is an epipolar stereo image, where corresponding points have the same vertical coordinates in both images, thus lie on the same scan-line. The objective of this module is to map the stereo images into a *virtual stereo image*, which have aligned viewing directions, identical image planes and parallel image coordinate systems.

Feature extraction: The `input` of the feature extraction is an epipolar stereo image without any distortions. The `output` of this module is a list of image points extracted in both stereo images. The determination of *significant* features is the basis for all following steps. Here, we use significant edge points as features, whereby a significant point is defined by the following useful requirements: the points should be sufficiently different to their neighborhood, invariant to geometrical and radiometrical transformations, seldom, interpretable, and the extraction of points should be insensitive to noise. The implemented algorithm is a one-dimensional version of the one published by (Förstner and Gülch, 1987).

Feature-based matching: The objective of this module is to find corresponding feature points in order to reconstruct their 3-D position. The `input` of the matching is the list of points of interest in both images. The `output` is a list of corresponding points with their similarity as additionally attribute. The matching is realized in two stages. Based on a list of candidate matches, i. e., putative corresponding points, using a similarity measure, determined in the first step, the correspondences are made unique by concictency checks in the second step. The resulting list obeys the principles of exclusiveness and similarity. Finally, the 3-D coordinates of the matched image points are determined by intersecting the image rays passing through the optical center and the image points.

Seat occupation detection: The `input` consists of the list of corresponding points. The `output` of this module is the decision whether the seats are empty or occupied. If a seat is classified as empty one obtains the form and position of the seat. In the case a seat is occupied we do not distinguish between passengers and any other objects. The *seat occupation detection* is the first module in our computational structure, which supplies usable information to an intelligent airbag deployment. The knowledge of position and form of driver and passenger seat facilitates the classification of seat occupation substantially. The selected seat model, an elliptical cylinder, can be easly replaced by more sophisticated one in order to improve the results if necessary. The developed procedure is described in details in (Faber, 2000).

Passenger detection and localization: The `input` is the list of corresponding points and the available information about the status of seat occupation. The `output` of the last module at the moment is defined by the information about a possible seat occupation by a human. Thereby, if a seat is occupied by a human, the information about position and orientation of the human's head as the most distinguishing feature of the body are available. The head is approximated by an ellipsoid, specified by geometrically interpretable parameters.

A detailed description of the developed procedure is given in the following section.

3 PASSENGER DETECTION AND LOCALIZATION

The detection and localization of passengers inside a vehicle is the most important step within an intelligent airbag deployment. On the basis of the determined position of a passenger inside the vehicle it should be possible to control the airbag deployment in the case of an accident directly.

3.1 Data

The shape of the human's head can be well approximated by a rigid, three-dimensional model because the head is nearly rigid and roughly symmetrical. The head is modeled by an ellipsoid as mentioned with the geometrical restrictions of a

human's head: the head length range between 192 and 257 [mm], the head height between 163 and 205 [mm] and the head breadth between 137 and 168 [mm], respectively to the DIN 33402/2 "Human body dimensions; values".

The available data are defined by the set of all corresponding points. That means, all points are potential candidates belonging to an ellipsoid describing the human's head. But, our main problem is, that the points are irregularly distributed in the 3-D space and, moreover, additionally no information about the relations between the points is available. The resulting problem is a defined selection of a subset of 3-D points, which are representative of the searched ellipsoid.

The detection is performed using a RANSAC procedure (Fischler and Bolles, 1981). Here, however, we need to randomly select nine points and check their validity. The best solution is then refined using a direct least squares method with a condition, which supports, but nor enforces the approximation of an ellipsoid. The least squares method is similar to the approach of (Fitzgibbon et al., 1996).

3.2 Ellipsoid specific fitting algorithm

A general second order surface can be present in 3-D implicitly $\mathbf{F}(\mathbf{z},\mathbf{x}) = \mathbf{x}\cdot\mathbf{A}\cdot\mathbf{x}^T + \mathbf{x}\cdot\mathbf{a} + a_{44} = 0$ with $\mathbf{a} = [a_{14}\ a_{24}\ a_{34}]^T$, $\mathbf{x} = [x\ y\ z]$ and the real symmetrical matrices

$$\mathbf{A} = \begin{pmatrix} a_{11} & a_{12} & a_{13} \\ a_{21} & a_{22} & a_{23} \\ a_{31} & a_{32} & a_{33} \end{pmatrix} \quad , \quad \mathcal{A} = \begin{pmatrix} a_{11} & a_{12} & a_{13} & a_{14} \\ a_{21} & a_{22} & a_{23} & a_{24} \\ a_{31} & a_{32} & a_{33} & a_{34} \\ a_{41} & a_{42} & a_{43} & a_{44} \end{pmatrix} .$$

Explicitly the general second order surface can be read as:

$$\mathbf{F}(\mathbf{z},\mathbf{x}) = a_{11}x^2 + a_{22}y^2 + a_{33}z^2 + 2a_{12}xy + 2a_{13}xz + 2a_{23}yz + a_{14}x + a_{24}y + a_{34}z + a_{44} = 0\ . \tag{1}$$

$\mathbf{F}(\mathbf{z},\mathbf{x}_i)$ is called the *algebraic distance* of a point $\mathbf{x}_i = [x_i\ y_i\ z_i]$ to the surface $\mathbf{F}(\mathbf{z},\mathbf{x}) = 0$. The fitting of a general surface may be approached (Haralick and Shapiro, 1993) by minimizing the sum of the squared algebraic distances:

$$\Delta = \sum_{i=1}^{n} \mathbf{F}\left(\mathbf{z},\mathbf{x}_i\right)^2 \rightarrow Minimum\ . \tag{2}$$

In order to avoid the trivial solution for the parameter, and recognizing that any multiple of a solution represents the same surface, the formulation of a constraint is necessary. The selection of a suitable constraint is important for the fitting. Note, if a constraint is selected which has insufficiently discriminant characteristics, a set of 3-D points can be fitted by an *ellipsoid*, a *hyperboloid*, a *double cone*, or any surface, which does not present a center surface. On the other hand, the equation to describe an ellipsoid can be written in a normalized form:

$$\frac{x^2}{A^2} + \frac{y^2}{B^2} + \frac{z^2}{C^2} = 1 \quad \text{with} \quad A > 0\ ,\ B > 0\ ,\ C > 0\ .$$

In order to fit ellipsoids specifically we would like to constrain the parameter vector $\mathbf{z}$. A constraint which forces the fitting of an ellipsoid always can be formulated as

$$\det\left(\mathbf{A}\right) = a_{11}a_{22}a_{33} + a_{12}a_{23}a_{31} + a_{13}a_{32}a_{21} - a_{11}a_{23}a_{32} - a_{22}a_{13}a_{31} - a_{33}a_{12}a_{21} = 1\ . \tag{3}$$

However, on the basis of the obvious structural contradiction between the actual formulation and the demanded structure to solve the generalized eigenvalue problem $\mathbf{Bz} = \lambda\mathbf{Cz}$ with $\mathbf{z}^T\mathbf{Cz} = 1$ and $z = [a_{11}\ a_{22}\ a_{33}\ a_{12}\ \ldots\ a_{44}]$ this formulation is not suitable. Concluding, a "good" approximation of the constraint has to been selected to exclude at least the surfaces, which do not present a center surface. Therefore it is necessary, that $\det\left(\mathbf{A}\right) \neq 0$. Assuming, that every projection of the 3-D point set into the three 2-D plane $X-Y$, $X-Z$, and $Y-Z$ are approximated optimal by an ellipse the following and finally used constraint is motivated:

$$4\left(a_{11}a_{22} + a_{11}a_{33} + a_{22}a_{33}\right) - \left(a_{12}a_{21} + a_{13}a_{31} + a_{23}a_{32}\right) = 1\ . \tag{4}$$

This is a quadratic constraint which may be expressed in the matrix form $\mathbf{z}^T\mathbf{Cz} = 1$ as

$$\mathbf{z}^T \cdot \begin{bmatrix} 0 & 2 & 2 & 0 & 0 & 0 & 0 & 0 & 0 & 0 \\ 2 & 0 & 2 & 0 & 0 & 0 & 0 & 0 & 0 & 0 \\ 2 & 2 & 0 & 0 & 0 & 0 & 0 & 0 & 0 & 0 \\ 0 & 0 & 0 & -1 & 0 & 0 & 0 & 0 & 0 & 0 \\ 0 & 0 & 0 & 0 & -1 & 0 & 0 & 0 & 0 & 0 \\ 0 & 0 & 0 & 0 & 0 & -1 & 0 & 0 & 0 & 0 \\ 0 & 0 & 0 & 0 & 0 & 0 & 0 & 0 & 0 & 0 \\ 0 & 0 & 0 & 0 & 0 & 0 & 0 & 0 & 0 & 0 \\ 0 & 0 & 0 & 0 & 0 & 0 & 0 & 0 & 0 & 0 \\ 0 & 0 & 0 & 0 & 0 & 0 & 0 & 0 & 0 & 0 \end{bmatrix} \cdot \mathbf{z} = 1.$$

Note, the fitting of an ellipsoid will be supported only, not forced, if this constraint is selected. Following Bookstein (Bookstein, 1979), the constrained fitting problem can be written as:

$$\Delta = \sum_{\substack{\mathbf{x}_i \\ i\in[1,n]}} \Big[a_{11}x_i^2 + a_{22}y_i^2 + a_{33}z_i^2 + 2a_{12}x_iy_i + 2a_{13}x_iz_i + 2a_{23}y_iz_i + a_{14}x_i + a_{24}y_i + a_{34}z_i + a_{44} \Big]^2 \rightarrow Minimum \tag{5}$$

subject to the constraint $\mathbf{z}^T\mathbf{C}\mathbf{z} = 1$. The numerical solution of the resulting non-linear equation system will be obtained by a quadratically constrained least squares minimization as proposed in (Gander, 1981). First, by applying the Lagrange multipliers we get the conditions for the solution of $\mathbf{z}$: $\mathbf{B}\mathbf{z} = \lambda\mathbf{C}\mathbf{z}$ with $\mathbf{z} = [a_{11}\ a_{22}\ a_{33}\ a_{12}\ a_{13}\ a_{23}\ a_{14}\ a_{24}\ a_{34}\ a_{44}]$, the matrix $\mathbf{B} = \mathbf{U}^T\mathbf{U}$ and the matrix

$$\mathbf{U} = \begin{bmatrix} x_1^2 & y_1^2 & z_1^2 & x_1y_1 & x_1z_1 & y_1z_1 & x_1 & y_1 & z_1 & 1 \\ x_2^2 & y_2^2 & z_2^2 & x_2y_2 & x_2z_2 & y_2z_2 & x_2 & y_2 & z_2 & 1 \\ \cdots & & & & & & & & & \\ x_i^2 & y_i^2 & z_i^2 & x_iy_i & x_iz_i & y_iz_i & x_i & y_i & z_i & 1 \\ \cdots & & & & & & & & & \\ x_n^2 & y_n^2 & z_n^2 & x_ny_n & x_nz_n & y_nz_n & x_n & y_n & z_n & 1 \end{bmatrix} .$$

Solving the generalized eigenvalue problem, we are looking for the eigenvector $\mathbf{z}_k$ corresponding to the minimal positive eigenvalue λ_k. Finally, after a proper scaling ensuring $(\mathbf{z}_k)^T\mathbf{C}(\mathbf{z}_k) = 1$, we get a solution of the minimization problem (Eq. 5) which represents the best-fit 2-D center surface in 3-D for the given point set.

3.3 Verification.

Now, in the step of verification we decide wether the obtained eigenvector represents the desired solution, from which geometrically interpretable parameters of the ellipsoid can be derived. Therefore, we use the standard measures respecting to the DIN 33402/2. Concretely, we refer to the values bounding between the 5th percentile female to the 95th percentile male of persons aged between 16 and 65. Secondly, we check, if the actual hypothesis is supported by additionally 3-D points. If the hypothesis is confirmed, we accept the fitted ellipsoid.

To derive geometrically interpretable parameters from the parameter vector $\mathbf{z}_k = [a_{11}\ a_{22}\ \ldots\ a_{44}]$ three different transformations are needed as given below:

1. Firstly, the coordinate system is moved by a translation vector $[\xi\ \eta\ \nu]^T$. And it is required, that the linear terms vanish:
$$\begin{aligned} &a_{11}(x_m+\xi)^2 + a_{22}(y+\eta)^2 + a_{33}(z+\nu)^2 + \\ &a_{12}(x_m+\xi)(y+\eta) + a_{13}(x_m+\xi)(z+\nu) + a_{23}(y+\eta)(z+\nu) + \\ &a_{14}(x_m+\xi) + a_{24}(y+\eta) + a_{34}(z+\nu) + a_{44} = 0\ . \end{aligned}$$
Now we can estimate the coordinates of the center:
$$\begin{aligned} x_m &= \frac{2\left(2a_{22}a_{33}a_{14} - a_{33}a_{12}a_{24} - a_{22}a_{13}a_{34}\right) + a_{23}\left(a_{12}a_{34} + a_{13}a_{24} - a_{23}a_{14}\right)}{2\left(4a_{11}a_{22}a_{33} + a_{12}a_{13}a_{23} - a_{11}a_{23}^2 - a_{22}a_{13}^2 - a_{33}a_{12}^2\right)} \\ y_m &= \frac{2\left(2a_{11}a_{33}a_{24} - a_{33}a_{12}a_{14} - a_{11}a_{23}a_{34}\right) + a_{13}\left(a_{12}a_{34} + a_{23}a_{14} - a_{13}a_{24}\right)}{2\left(4a_{11}a_{22}a_{33} + a_{12}a_{13}a_{23} - a_{11}a_{23}^2 - a_{22}a_{13}^2 - a_{33}a_{12}^2\right)} \\ z_m &= \frac{2\left(2a_{11}a_{22}a_{34} - a_{22}a_{13}a_{14} - a_{11}a_{23}a_{24}\right) + a_{12}\left(a_{13}a_{24} + a_{23}a_{14} - a_{12}a_{34}\right)}{2\left(4a_{11}a_{22}a_{33} + a_{12}a_{13}a_{23} - a_{11}a_{23}^2 - a_{22}a_{13}^2 - a_{33}a_{12}^2\right)}\ . \end{aligned}$$
The resulting equation of the ellipsoid in the shifted $\xi - \eta - \nu$ coordinate system is:
$$\begin{aligned} (\xi\ \eta\ \nu)\,\mathbf{M}\begin{pmatrix}\xi\\ \eta\\ \nu\end{pmatrix} &= (\xi\ \eta\ \nu)\begin{pmatrix} a_{11} & a_{12}/2 & a_{13}/2 \\ a_{12}/2 & a_{22} & a_{23}/2 \\ a_{13}/2 & a_{23}/2 & a_{33}\end{pmatrix}\begin{pmatrix}\xi\\ \eta\\ \nu\end{pmatrix} \\ &= a_{11}\xi^2 + a_{22}\eta^2 + a_{33}\nu^2 + a_{12}\xi\eta + a_{13}\xi\nu + a_{23}\eta\nu = h\ , \end{aligned}$$
with
$$h = a_{11}x_m^2 + a_{22}y_m^2 + a_{33}z_m^2 + a_{12}x_my_m + a_{13}x_mz_m + a_{23}y_mz_m + a_{14}x_m + a_{24}y_m + a_{34}z_m + a_{44}\ .$$

2. The positiv eigenvalues of the symmetrical matrix $\mathbf{M}$ are estimated by a main axes transformation. Then, the equation of the ellipsoid is transformed by a rotation in the standard form:

$$\lambda_1 (\xi)' + \lambda_2 (\eta)' + \lambda_3 (\nu)' = h$$

   Now, the length of the three main axes can be estimated:

$$A = \sqrt{\frac{h}{\lambda_1}} \ , \quad B = \sqrt{\frac{h}{\lambda_2}} \ , \quad C = \sqrt{\frac{h}{\lambda_3}} \, .$$

3. Finally, the angles specifying the orientation of the elliposid in the 3-D space are estimated on the basis of the components of the eigenvector Λ_1 corresponding to the largest eigenvalue λ_1 related to the ξ axis.

$$\alpha = \arccos (\Lambda_1(\xi)) \ , \quad \beta = \arccos (\Lambda_1(\eta)) \ , \quad \gamma = \arccos \left(\Lambda_(\nu)1\right)$$

The verification of the actual hypothesis is mainly realized on the basis of the estimated geometrically interpretable parameters A, B, and C. The other estimated parameters are not suitable in this validation step, because the position and the orientation of the ellipsoid approximating the human's head can vary within wide bounds. Assuming, that the lenghts of the main axes of the fitted ellipsoid are within the intervals for the head length, the head height and the head breadth and more than l 3-D points support the hypothesis without that more than k 3-D points are inside the fitted ellipsoid, the fitting will be accepted.

4 EXPERIMENTS

The described computational structure can be used a) to detect and classify the seats, and b) to detect and localize passengers inside a vehicle. To demonstrate the performance of the structure the performance of the single modules were characterized analyzing numerous image sequences. However, in the following section we firstly sketch the practical realization of the used fitting algorithm and in section 4.2 we demonstrate the feasibility of the approach.

4.1 Practical realization of the ellipsoid specific fitting algorithm.

The improved fitting algorithm was implemented in the same straightforward way as the original Fitzgibbon's method (Fitzgibbon et al., 1996). The appropriate MATLAB code proposed by the author is:

```
% ellipsoid fitting, (x,y,z) are lists of coordinates
function a=fit_ellipsoid(x,y,z)
% build the 10×10 constraint matrix
C(10,10)=0;
C(1,2)=2; C(2,1)=2; C(4,4)=-1;
C(1,3)=2; C(3,1)=2; C(5,5)=-1;
C(2,3)=2; C(3,2)=2; C(6,6)=-1;
% build the design matrix
D=[x.^2 y.^2 z.^2 x.*y x.*z y.*z x y z ones(size(x))];
% build the scatter matrix
S=D'*D;
% solve the constrained eigensystem
[gevec,geval]=eig(C,S);
% find the eigenvector for the minimum positive eigenvector
[posr,posc]=find(geval > 0 & ~isinf(geval));
% extract the corresponding eigenvector
a=gevec(:,posc);
```

4.2 Experimental results

In fig. 4 and fig. 5 the results for two example frames of two different sequences are sketched for every computational step. The rectification of the images a) and b) eads to the epipolar images c) and d). The difference is particularly visible e. g. in the four corners. The extracted feature points sketched in e) and f) show the dependency of the density on the local varibility of the brightness in the images, especially in homogeneous areas no feature points are found. The matched points in g) and h) show the projection of the sparse depth map into the images.

In fig. 4 i) + j) the occupancy test correctly classified the driver seat as empty, the passenger seat was identified as occupied and thus a seat model cannot be fitted. In fig. 5 i) + j) the situation is reversed, also reflecting a correct decision

by the model *seat occupation detection*. In fig. 5 k) + l) the projection of the 3-D point set forming the approximation of a sucessfully approximated human's head is sketched. Assuming, that the approximation is correct, we can use the determined parameter of the ellipsoid to control the airbag deployment. The parameter set of the sketched ellipsoid are: $x_m = 294.56$ mm, $y_m = 302.25$ mm, $z_m = -579.66$ mm, and $A = 116.92$ mm, $B = 94.24$ mm, $C = 76.78$ mm corresponding the the head length $2 \cdot A$, head height $2 \cdot B$ and head breadth $2 \cdot C$ (cf. the values in section 3.1).

The reliability of the results of the module *seat occupation detection* is very high. If a seat is occupied by a human (or any significant object) in reality it is always classified as occupied. The reliability of the results of the module *passenger detection and localization* shows some weak points up. Thus e.g. the "plausible" possibility of the approximation of a shoulder or the head restraint exists as human's head. Likewise the reliability of a reliable detection causes difficulties. In these cases the justified assumption exists that a sequence processing brings the desired stability.

5 CONCLUSION

The presented results show that the objective, the detection and localization of passengers inside vehicles, can be reached using the described computational structure. If a seat is occupied by a human it is possible to detect and localize the human's head as the most distinguished part of the body.

The achievable results then can give the necessary information *wether* and *how* an airbag has to be deployed in the case of an accident to protect the passengers inside a vehicle against heavy violations.

REFERENCES

The National Highway Traffic Safety Administration, 1999. Airbags. `http://www.nhtsa.dot.gov`.

The Insurance Institute for Highway Safety, 1996. Airbags. `http://www.highwaysafety.org`.

Aggarwal, J. K. and Cai, Q., 1999. Human motion analysis: A review. CVIU 73(3), pp. 428–440.

Birchfeld, S., 1998. Elliptical head tracking using intensity gradients and color histograms. In: CVPR.

Bookstein, F. L., 1979. Fitting conic sections to scattered data. Computer Graphics and Image Processing 9, pp. 56–71.

Faber, P., 2000. Seat occupation detection inside vehicles. In: Proc. Southwest Symp. on Image Analysis and Interpretation.

Fieguth, P. and Terzopoulos, D., 1997. Color-based tracking of heads and other mobile objects at video frame rates. In: CVPR.

Fischler, M. A. and Bolles, R. C., 1981. Random sample consensus: A paradigm for model fitting with applications to image analysis and automated cartography. Comm. of the ACM 24(6), pp. 381–395.

Fitzgibbon, A. W., Pilu, M. and B.Fisher, R., 1996. Direct least squares fitting of ellipses. Technical report, Univerity of Edinburgh.

Förstner, W. and Gülch, E., 1987. A Fast Operator for Detection and Precise Location of Distrinc Points, Corners and Centres of Circular Features. In: Intercommision Conference of ISPRS on Fast Processing of Photogrammetric Data.

Gander, W., 1981. Least squares with a quadratic constraint. Numerische Mathematik 36, pp. 291–307.

Gavrila, D. M., 1999. The visual analysis of human movement: A survey. CVIU 73(1), pp. 82–98.

Haralick, R. M. and Shapiro, L. G., 1993. Computer and Robot Vision. Vol. 2, Addison-Wesley.

Krumm, J. and Kirk, G., 1998. Video occupant detection for airbag deployment. In: 4th IEEE Workshop on Applications of Computer Vision.

Schubert, A. and Dickmanns, E. D., 1998. Real-time gaze observation for tracking human control of attention. In: Face Recognition: From theory to Applications, Springer, pp. 617–626.

Sobottka, K. and Pitas, I., 1996. Segmentation and tracking of faces in color images. In: 2nd Int. Conf. on Automatic Face and Gesture Recognition.

Yow, K. C. and Cipolla, R., 1996. Feature-based human face detection. Technical report, University of Cambridge.

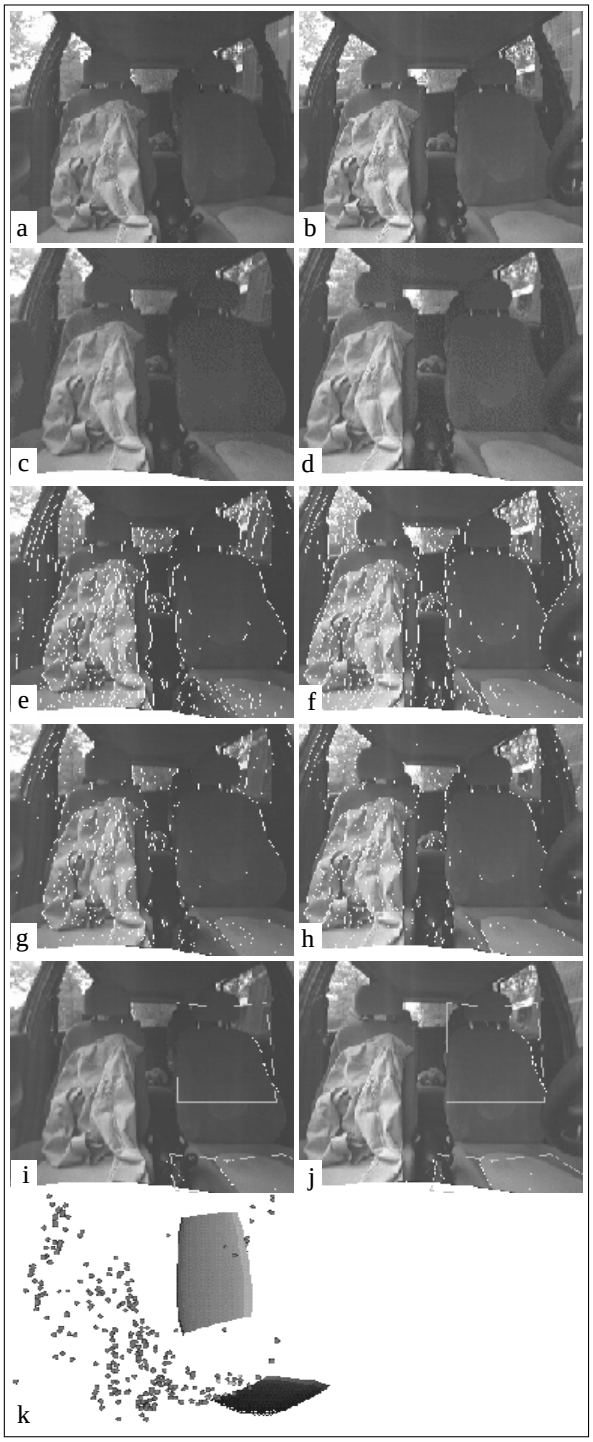

Figure 4: Results for the 1st frame of SEQ_3: a) + b) left and right stereo image, c) + d) epipolar stereo images, e) + f) extracted points of interest, g) + h) matched points, i) + j) sketched seat approximation, k) snapshot of the generated VRML file (only the driver seat is modeled as the passenger seat is classified as occupied).

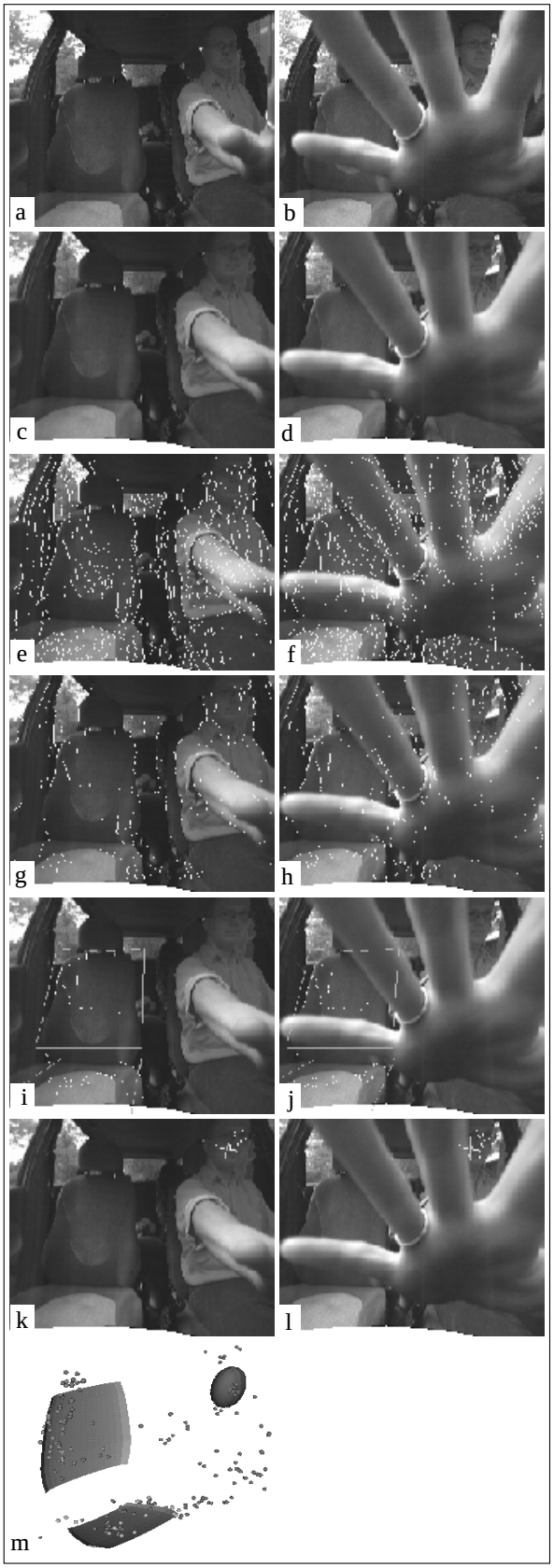

Figure 5: Results for the 1st frame of SEQ_2: a) + b) left and right stereo image, c) + d) epipolar stereo images, e) + f) extracted points of interest, g) + h) matched points, i) + j) sketched seat approximation, k) + l) sketched human's head approximation, m) snapshot of the generated VRML file.